A COMPARISON BETWEEN FAST FACTORIZED BACKPROJECTION AND FREQUENCY-DOMAIN ALGORITHMS IN UWB LOWFREQUENCY SAR

Viet T.Vu, Thomas K. Sjögren, Mats I. Pettersson

Department of Signal Processing, Blekinge Institute of Technology
PO Box 520, 37225 Ronneby, Sweden
phone: + (46) 708610395, fax: + (46) 45727914, email: viet.thuy.vu@.bth.se

ABSTRACT

Two frequency-domain algorithms Chirp Scaling (CS) with the advantage of simplification and Range Migration (RM) with the advantage of accuracy are candidates for a comparative study to the time-domain algorithm Fast Factorized Backprojection (FFBP) with reference to a UWB system are presented in this paper. The comparison is based on UWB SAR image quality measurements such as spatial resolution, Integrated Sidelobe Ratio (ISLR), Peak Sidelobe Ratio (PSLR) and processing time connected to computational cost. The simulated SAR data, which is used in this study, is based on the parameters of the airborne UWB low frequency CARABAS-II system.

Index Terms— Comparison, FFBP, RM, CS, UWB, SAR

1. INTRODUCTION

Different algorithms have been proposed to process SAR images. The main objectives of algorithms are image quality, time consumption connected to computational cost and other aspects related to application. SAR image processing algorithm can be divided into two main groups: time-domain and frequency domain algorithms. Global Backprojection (GBP) algorithm [1] is known as the basic of the time-domain algorithms to reconstruct the image scene. According to GBP, a SAR image is considered as a linear transformation from the radar echo data and can be considered to be a reference SAR image in UWB SAR image quality measurements. The main disadvantage of GBP which exists parallel with advantages of GBP such as perfect motion compensation, unlimited scene size, prefect focus and local processing is computation cost. For N aperture points and SAR image of N by N pixels, the number of operations needed for GBP is proportional to N^3. Fast time-domain algorithms were proposed to overcome the drawback of the GPB, for example Local Backprojection (LBP) [2] and Fast Factorized Backprojection (FFBP) [3] running roughly $N^2\sqrt{N}$ and $N^2\log(N)$ times faster than GBP, respectively. Range Migration algorithm (RM) [4], Range-Doppler (RD) [5] and Chirp Scaling (CS) [6] are examples of frequency-domain algorithms. Both RM and RD require computationally expensive interpolation while among CS algorithm avoids interpolation and can be efficiently performed by complex multiplications and Fast Fourier Transforms (FFT). However, in derivations of both CS and RD, high order phase terms in some steps are discarded. For this reason, RM may be the most suitable frequency-domain algorithm for UWB low frequency SAR systems.

In comparative studies between algorithms, either time-domain algorithms or frequency-domain algorithms are usually compared together. For example, a comparison of different FFBP versions is presented in [7]. In [8], a comparison of CS and RM for airborne low frequency SAR data processing is given. Another comparative study of RD and RM algorithms concentrates on focusing quality can be found in [9]. However, there have not been many comparisons between time-domain and frequency-domain algorithms even though they form two main SAR processing algorithm groups.

In this paper, two frequency-domain algorithms including CS with the advantage of simplification and RM with the advantage of accuracy are candidates for a comparative study to a fast time-domain algorithm FFBP using simulated CARABAS-II data [10]. The comparison is based on UWB SAR image quality measurements such as spatial resolution, Integrated Sidelobe Ratio (ISLR) and Peak Sidelobe Ratio (PSLR) [11] and processing time connected to computational complexity.

The paper is organized as follows: Section 2 describes briefly different algorithms. Theory of SAR image quality measurements is presented in Section 3. A comparative study of different algorithms is given in Section 4. Section 5 provides the conclusions.

The authors would like to thank the colleagues at the Swedish Defence Research Agency for the CARABAS-II SAR data supplied in this research. The authors would also like to thank the KK-Foundation for making this research project possible, and the support from Saab Bofors Dynamics, Saab Microwave Systems and Saab Space.

2. ALGORITHMS TO PROCESS UWB SAR DATA

2.1. Fast Factorized Backprojection

The subimage based version of FFBP [3, 7] can be interpreted as LBP [2] processing data in multiple beamforming stages so-called factorization. For FFBP, the range compressed data is mapped into first order beams. The beams are formed by short first order subaperture and the beam size should be large to cover the first order large images. A number of first order beams are combined together to form a second order beam corresponding to the combination of a number of first order subapertures. The size of second order beam is smaller and covers the second order subimages which are created by the division of the first order subimages. Beamforming stages are repeated until the final beamforming stage. The number of beamforming stages or factorizations depends strongly on SAR system parameters, required image quality and processing time. In the final stage, the subimages are mapped by beams formed at the final beamforming stage. A full SAR image is obtained by a coherent combination of all subimages processed by the full aperture.

2.2. Range Migration

RM enables to reconstruct the image of large scenes at fine resolution. RM requires the so-called Stolt interpolation which can be interpreted as a change of variables in the frequency domain by the relationship [4]

$$\omega = \frac{\mathrm{c}}{2}\sqrt{k_x^2 + k_r^2} \tag{7}$$

where ω is the signal frequency, k_x and k_r are wavenumbers in azimuth and range, respectively. The focusing equation of RM can be rewritten as

$$h(x, r, -t_0) = \frac{\mathrm{c}}{8\pi^2}\iint G'(k_x, r=0, k_r)\ \frac{k_r}{\sqrt{k_x^2 + k_r^2}} \exp\left\{-\mathrm{j}\frac{\mathrm{c}t_0}{2}\sqrt{k_x^2 + k_r^2}\right\} \cdot \exp\{\mathrm{j}(k_x x + k_r r)\}\ \mathrm{d}k_x \mathrm{d}k_r \tag{8}$$

where $G'(k_x, r=0, k_r)$ is measured field which has been changed variable at $r=0$ of the superposition of plane waves with different wavelengths and azimuth wavenumbers in two-dimensional frequency domain at the emitted time $-t_0$.

2.3. Chirp Scaling

Approximations in derivation of the original CS [6] by Taylor expansion to second order are valid for conventional narrow band SAR systems but might not completely valid for UWB systems associated with large integration angle. A conventional approach to such a problem is to introduce a Taylor expansion up to higher order phase terms and take spatial variant range migration into account. Nonlinear CS (NCS) proposed in [12] with the consideration up to cubic phase terms for Taylor expansion combined with cubic order nonlinear chirp rate to process squint mode SAR data is therefore a candidate to process UWB mode SAR data. According to NCS [12], the range frequency rate K_r is assumed to vary linearly with the range-time from reference trajectory

$$K_r \approx K_{r,\mathrm{ref}} + K_s \frac{2(r_0 - r_{\mathrm{ref}})}{\mathrm{c}\beta} \tag{1}$$

where r_0 and r_{ref} are minimum range distance to a point target and reference range, respectively. β is a function of azimuth frequency f_x and defined in [6] as

$$\beta = \sqrt{1 - \left(\frac{\mathrm{c}f_x}{2f_{\mathrm{c}}v_{\mathrm{pl}}}\right)^2} \tag{2}$$

An extra cubic phase filter is performed in two-dimensional (2-D) frequency domain by

$$H_{\mathrm{Cubic}} = \exp\left\{\mathrm{j}\frac{2\pi}{3}\left[\frac{K_s(2-\beta)}{2K_{r,\mathrm{ref}}^3(1-\beta)} - \frac{3r_0}{\mathrm{c}f_{\mathrm{c}}^2}\frac{\beta^2 - 1}{\beta^5}\right]\right\} \tag{3}$$

References functions including chirp scaling, range compression and residual error compensation functions are

$$H_{\mathrm{CS\_3}} = H_{\mathrm{CS\_2}} \cdot \exp\left\{\mathrm{j}\pi\frac{1}{3}K_s\left(\frac{1}{\beta} - 1\right)\left(\tau - \frac{2r_{\mathrm{ref}}}{\mathrm{c}\beta}\right)^3\right\} \tag{4}$$

$$H_{\mathrm{RC\_3}} = H_{\mathrm{RC\_2}} \cdot \exp\left\{\mathrm{j}\frac{\pi(1+\beta)}{3f_{\mathrm{c}}K_{r,\mathrm{ref}}}f_r^3\right\} \tag{5}$$

$$H_{\mathrm{RES\_3}} = H_{\mathrm{RES\_2}} \cdot \exp\left\{\mathrm{j}\frac{\pi K_{r,\mathrm{ref}}^2}{3f_{\mathrm{c}}}\frac{(1-\beta)^2(1+\beta)}{\beta^5}\right\} \tag{6}$$

where $H_{\mathrm{CS\_2}}$, $H_{\mathrm{RC\_2}}$ and $H_{\mathrm{RES\_2}}$ are the reference functions of original CS which can be found in [6].

3. SAR IMAGE QUALITY MEASUREMENTS

Analyses in [11] have shown that the mainlobe and sidelobe areas are more suitably defined by ellipses. Base on these analyses, definitions on SAR image quality measurement such as Integrated Sidelobe Ratio (ISLR) and Peak Sidelobe Ratio (PSLR) have been proposed. Due to the fact that UWB SAR system is always associated with large integration angle to handle azimuth focusing, investigations of spatial resolution, ISLR and PSLR under different integration angles are also proposed in [11]. Spatial resolution which is considered to be the most significant parameter in SAR image quality measurements, ISLR and PSLR are used to evaluate quantitatively the performance of the algorithms mentioned in Section 2.

Table 1. CARABAS-II's main parameters

Parameter	*Value*
The highest frequency processed	82.5 MHz
The lowest frequency processed	21.785 MHz
Platform speed v_{pl}	128 m/s
Flight altitude	3700 m
Minimum range	7150 m
Pulse Repetition Frequency (PRF)	137Hz

The spatial resolutions are measured by the 3dB beamwidth δ_x and δ_r in azimuth and range of the impulse response function of a point target. ISLR is defined by the ratio of the energy within the sidelobe area bounded by concentric ellipses ($2\delta_x$, $2\delta_r$) and ($10\delta_x$, $10\delta_r$) to the energy of mainlobe area bounded by ellipse ($2\delta_x$, $2\delta_r$). The ratio of the peak intensity found within sidelobe area to the one found within mainlobe areas defines PSLR.

4. COMPARATIVE STUDIES

The simulated data which is used in this study is based on parameters of the CARABAS-II system given in Table 1. To obtain a fair comparison, no weighting function or sidelobe control approach is used. With the CARABAS-II parameters given in Table 1, we can consider the integration angles in the range from 5 to 70 degrees in this comparative study according to [11]. Three algorithms FFBP, RM and NCS are subjects to be compared. However, not all of these algorithms are completely valid for CARABAS-II data processing and this can be explained as follows. In SAR system design, the PRF must be chosen larger or equal to two time maximum Doppler frequency which is a function of maximum integration angle and signal fractional bandwidth. For CARABAS-II, high PRF with regard to extremely large integration angle (up to 150 degrees) may make both original CS and NCS invalid since the term β may get complex values at certain azimuth frequencies. Neither FFBP nor RM suffers from such problem. For comparison purposes, the data is simulated with low PRF (only 68.5 Hz instead of 137 Hz).

For NCS, we need to eliminate azimuth-range coupling [12, 13] mainly caused by Higher Order Phase (HOP) terms (from 4^{th} order) in the Taylor expansion due to extremely high fractional bandwidth of CARABAS-II (up to 1.16) Figure 1.c shows the degrading of the SAR image quality without HOP term elimination.

Nearest neighbor interpolator is used in both RM and FFBP in change of variable and beam forming stages after 10 times upsampling data, respectively. For FFBP, we process the data in 3 stages with the aperture block size $16 \times 4 \times 4$ and the same range and azimuth factorization $4 \times 4 \times 4$ for original image 256×256 pixels. Such parameters ensure the phase error to be smaller than $\pi/8$ (far field condition). Figure 1.a, 1.b and 1.d show the contour plots of a point target processed by FFBP, RM and NCS.

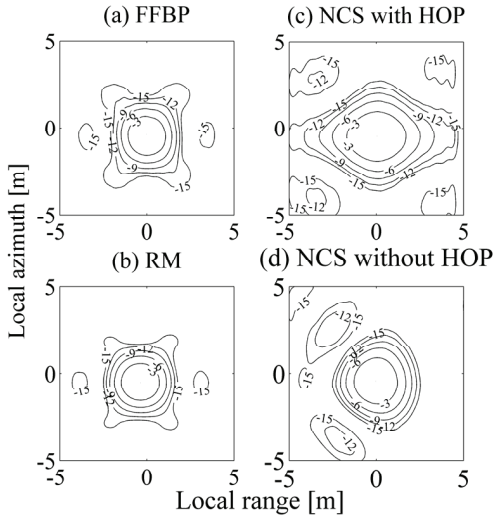

Fig. 1. The contour plots of a point target processed by different algorithms at integration angle of 35 degrees. Level steps from 0 to -15 dB are taken into account.

At the first glance, a better image quality is obtained by FFBP and RM than by NCS at a large integration angle. Measured spatial resolutions which are interpreted to be the distance between two objects on the ground at which the objects appear distinct and separate on SAR images are shown in Figure 2.a. Although NCS enables good resolutions at small integration angles, this does not hold at large integration angles (from 20 degrees). The measurement results of ISLR in Figure 2.a show again the worse performance of NCS at large integration angles when much more energy spills over to the sidelobes compared to RM and FFBP. Figure 2.b shows the high sidelobe level of NCS even at small integration angles which may be explained by phase errors caused by approximation in derivation steps of NCS and the extremely high fractional bandwidth in range. This leads to poor ability of NCS to image weak reflective targets affected by a strong reflective target nearby. NCS may therefore not be totally suitable for UWB SAR processing. If there is no motion error, RM can obtain the same SAR image quality as FFBP.

A comparison in term of processing time connected to computational complexity may be hard to be performed in an analytic way due to different basic operations used in time-domain and frequency-domain algorithms. For RM and NCS, operations which are mainly used are FFT, IFFT and multiplication while among FFBP uses only addition and multiplication. In our experiments performed by Matlab, at integration angles from 5 to 45 degrees, NCS shows the best performance in term of the processing time since NCS can be performed efficiently by FFT/IFFT and multiplications and does not require any interpolation. The processing time due to small data matrices corresponding to these integration angles does not get affected by extra steps required by NCS such as cubic phase filter and HOP elimination performed in 2-D frequency-domain.

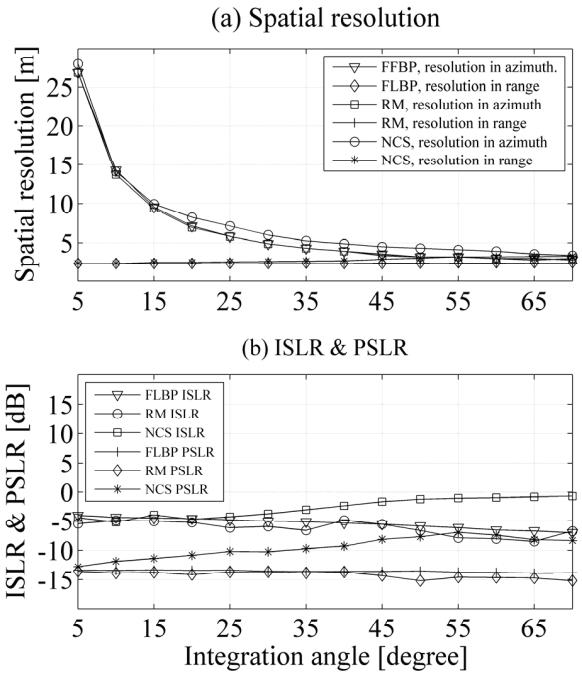

Fig. 2. SAR image quality measurements.

Bigger data matrices increasing proportional to larger integration make computational cost of NCS increase rapidly. While among with a simple interpolator such as a linear one, the computational cost of RM can be kept smaller than NCS at large integration angles. Both RM and NCS require much more memory than FFBP in SAR data processing. Computational cost will increase further for both RM and NCS if motion compensation is included.

FFBP processing time depends strongly on number of image pixels and on factorization parameters as mentioned in Section 2. A very small area, for example the 256×256 pixel image in our experiment, can be selected and in this case the computational cost is extremely small for FFBP. For large areas such as the SAR image processed in [3] with 6400×8192 pixels, the computational cost increases significantly. The selection of factorization parameters will decide the phase error for FFBP and therefore decide the SAR image quality. The processing time can be reduced by large subimages and long subapertures i.e. large phase error.

5. CONCLUSION

Algorithms FFBP, RM and NCS are subjects to be compared in this study. FFBP works perfectly with UWB SAR data. Processing time for FFBP depends strongly on image size and SAR image quality. If there is no motion error caused by airborne SAR systems, RM is an excellent candidate for UWB SAR processing in terms of SAR image quality and processing time. The study shows also that NCS may not be totally suitable for UWB SAR processing due to low image quality at large integration angles (from about 20 degrees) and long processing time (from about 45 degrees).

6. REFERENCES

[1] L. E. Andersson, "On determination of a function from spherical averages," *SIAM Journal on Mathematical Analysis*, vol.19, pp. 214–341, Jan. 1988.

[2] O. Seger, M. Herberthson, and H. Hellsten, "Real time SAR processing of low frequency ultra wide band radar data," *European Conference on Synthetic Aperture Radar*, pp. 489–492, May 1998.

[3] L. M. H. Ulander, H. Hellsten, and G. Stenstrom, "SAR processing using fast factorized backprojection," *IEEE Trans. on Aerospace and Electron. Syst*., vol. 39, pp. 760–776, July 2003.

[4] J. R. Bennett and I. G. Cumming, "A digital processor for the production of Seasat SAR imagery," *Proc. Internl. Conf. On Seasat-SAR Processor*, Dec. 1979.

[5] C. Cafforio, C. Prati, and F. Rocca, "SAR data focusing using seismic migration and techniques," *IEEE Trans. on Aerospace Electron. Syst*., vol. 27, pp. 194–207, Mar. 1991.

[6] R. K. Raney, H. Runge, R. Bamler, I. G. Cumming, and F. H.Wong, "Precision SAR processing using chirp scaling," *IEEE Trans. on Geosci. and Remote Sensing*, vol. 27, pp. 786–799, July 1994.

[7] T. K. Sjögren, V. T. Vu, and M. I. Pettersson, "A comparative study of the polar version with the subimage version of FFBP in UWB SAR," *Internl. Radar Symposium*, pp. 156–159, May. 2008.

[8] A. Potsis, A. Reigber, E. Alivizatos, A. Moreira, and N. K. Uzunoglou, "Comparison of chirp scaling and wavenumber domain algorithms for airborne low-frequency SAR," *Proc. of SPIE*, *SAR Image Analysis*, *Modeling, and Techniques* V, vol. 4883, pp. 11–19, Mar. 2003.

[9] R. Bamler, "A comparison of range-doppler and wavenumber domain SAR focusing algorithms," *IEEE Trans. on Geosci. and Remote Sensing*, vol. 30, pp. 706–713, July 1992.

[10] A. Gustavsson, L. M. H. Ulander, B. H. Flood, P.-O. Frolind, H. Hellsten, T. Jonsson, B. Larsson, and G. Stenstrom, "Development and operation of an airborne VHF SAR system-lessons learned," *IEEE Internl. Geosci. and Remote Sensing Symp. Proc*., vol. 1, pp. 458–462, July 1998.

[11] V. T. Vu, T. K. Sjögren, and M. I. Pettersson, "Definitions on SAR image quality measurement for UWB SAR," *SPIE Europe Remote Sensing*, UK, Sept. 2008. (*Accepted to be published as conf. proc.*)

[12] G. W. Davidson, I. G. Cumming, and M. R. Ito, "A chirp scaling approach for processing squint mode SAR data," *IEEE Trans. on Aerospace and Electron. Syst*., vol. 32 (11), pp. 121–133, Jan. 1996.

[13] Wang Jian, Xue Guoyi, Zhou Zhimin and Song Qian, "A new subaperture nonlinear chirp scaling algorithm for real-time UWB-SAR imaging," *Internl. Conf. on Radar 2006*, pp. 1–4, Oct. 2006.